SEARCHES FOR CHARGED HIGGS BOSONS AND SUPERSYMMETRY AT CDF*

BRENDAN BEVENSEE

Department of Physics and Astronomy
University of Pennsylvania, 209 S. 33rd St.,
Philadelphia, PA 19104, USA
Email: bevensee@upenn5.hep.upenn.edu

for the

CDF COLLABORATION

We present results of supersymmetric (SUSY) particle searches from the Collider Detector at Fermilab (CDF). First we describe searches for a charged Higgs boson and a stop squark, which could be produced in top quark decays. We also search for chargino-neutralino production using a trilepton signature. Finally, we investigate R-parity violating squark and LSP decay modes which have been proposed to accommodate the excess of high-Q^2 events at HERA. No evidence for SUSY is found, and limits are placed on these processes.

1. Introduction

We perform searches for supersymmetric (SUSY) particles using 110 pb^{-1} of $p\bar{p}$ collisions at the center-of-mass energy of $\sqrt{s}$ = 1.8 TeV, recorded by the Collider Detector at Fermilab (CDF) between 1992 and 1995. First, we describe searches for a charged Higgs boson ($H^{\pm}$) and a light stop squark ($\tilde{t}_1$) which could be produced in top quark decays. The large top quark mass of $M_{\rm top} = 175$ GeV/c^2 allows us to probe a mass range for the $H^{\pm}$ and the $\tilde{t}_1$ which would be inaccessible if these particles were only produced directly in $p\bar{p}$ collisions. Next, we describe a search for chargino-neutralino ($\tilde{\chi}_1^{\pm}\tilde{\chi}_2^0$) production using a trilepton signature, which has a small standard model (SM) background. Finally, we investigate a model which predicts the existence of R-parity violating ($\not{R}_{\rm p}$) squark production and decay to explain the excess of high-Q^2 events at HERA. An R-parity violating LSP ($\tilde{\chi}_1^0$) decay mode is also investigated. Both of these $\not{R}_{\rm p}$ decays would result in a like-charge dilepton signature.

Notable omissions to this talk include searches for squarks and gluinos using missing energy + jets final states [1] or like-charge dilepton final states [2], as well as SUSY searches which are motivated by the observation of an anomalous event with two high-P_T electrons, two high-P_T photons, and missing energy ($\not\!\!E_{\rm T}$) which was observed at CDF in April 1995 [3]. Searches for neutral Higgs bosons are discussed in reference [4].

The CDF detector, described in detail in reference [5], consists of tracking detectors which are located inside a 1.4 Tesla superconducting solenoid magnet, surrounded by calorimeters and muon chambers. To suppress

*Expanded version of conference proceedings submitted to the International Workshop on Quantum Effects in the MSSM, Universitat Autònoma de Barcelona, Barcelona, Spain, 9-13 September 1997.

background in our $t \to H^{\pm}b$ and $t \to \tilde{t}_1\tilde{\chi}_1^0$ searches, we identify b quarks by reconstructing secondary vertices from b decays with a silicon vertex detector (SVX), which is positioned immediately outside the beampipe. At least one secondary vertex (SVX b-tag) is detected in $(39 \pm 3)\%$ of all SM $t\bar{t}$ decays [6]. To search for LSPs which may be produced in SUSY particle decays and escape detection, we measure missing energy in the plane transverse to the beam ($\not\!\!E_{\rm T}$) with a resolution of approximately $0.7\sqrt{\Sigma E_T}$, where ΣE_T is the sum of transverse energy recorded in an event.

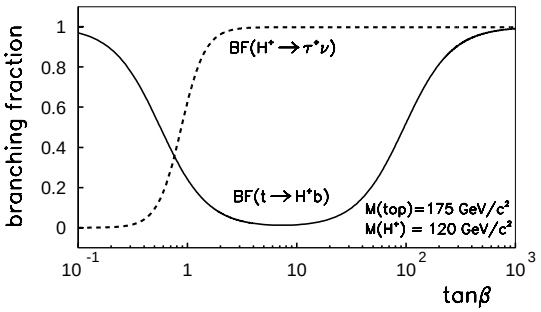

Figure 1: Branching fractions of the top quark and the charged Higgs boson as a function of tanβ, for $M_{H^{\pm}} = 120$ GeV/c^2.

2. Searches for charged Higgs bosons

Many SUSY models predict the existence of two Higgs doublets where one doublet couples to the up-type quarks and neutrinos, and the other couples to the down-type quarks and charged leptons [7]. In these theories, electroweak symmetry breaking produces five Higgs bosons, three of which are neutral and two of which are charged ($H^{\pm}$).

At the Fermilab Tevatron, if $M_{H^{\pm}} + M_b < M_{\rm top}$, then the primary mechanism for charged Higgs production is the top decay $t \to H^{\pm}b$, which competes with the SM decay $t \to W^{\pm}b$. The ratio of vacuum expectation values of the two Higgs doublets, tanβ, determines the dominant decay mode for the top quark and the $H^{\pm}$ (Figure 1). We expect to be sensitive to a large top quark branching fraction $\mathcal{B}(t \to H^{\pm}b)$, corresponding to the regions tan$\beta < 1$, where the decay $H^{\pm} \to cs$ dominates, and also tan$\beta > 50$, where $H^{\pm}$ decays exclusively to $\tau\nu$.

We use two methods to search for $H^{\pm}$. The first method is a direct search for $t\bar{t}$ events which contain one or two $H^{\pm} \to \tau\nu$ decays, for large values of tanβ [8]. The second method is an indirect search which uses the results of our top counting experiments to set limits for small and large values of tanβ.

2.1. *A direct search for $H^{\pm} \to \tau\nu$ in $t\bar{t}$ events at large tanβ*

For tan$\beta > 100$, often both top quarks in a $t\bar{t}$ event decay via $t \to H^{\pm}b \to \tau\nu b$, producing final states with two tau leptons, two b-quarks, and $\not\!\!E_{\rm T}$. For $30 <$ tan$\beta < 100$, $t\bar{t}$ frequently decays to $WbH\bar{b}$, resulting in a final state with one tau lepton, two b-quarks, $\not\!\!E_{\rm T}$, and the decay products from a $W^{\pm}$ boson.

Candidate events must have one of two distinctive topologies. The first topology is a "$\tau jjX + \not\!\!E_{\rm T}$" final state, where the τ lepton decays hadronically, "j" is a jet, and "X" is a jet or a lepton (e, μ, or τ). At least one of the jets must originate from a displaced vertex (SVX b-tag). The second topology is designed to select $t\bar{t} \to HbH\bar{b}$ events for a $M_{H^{\pm}}$ which is close to $M_{\rm top}$. A $\tau\tau + \not\!\!E_{\rm T}$ signature is expected, since the b-jet energies in these events often fall below the jet E_T requirement of the $\tau jjX + \not\!\!E_{\rm T}$ topology.

For the $\tau jjX + \not\!\!E_{\rm T}$ final state, one tau lepton must have $E_T > 20$ GeV, while any other tau lepton is required to have $E_T > 10$ GeV. Jets must have an uncorrected $E_T > 10$ GeV. For the ditau final state, both tau leptons must have $E_T > 30$ GeV. To reduce $Z \to \tau\tau$ background, they must not be opposite in azimuth ($\Delta\phi_{\tau\tau} < 160^0$). Both final

state topologies require $\not\!\!E_T > 30$ GeV. If the $\not\!\!E_T$ arises due to jet mismeasurement, usually the $\not\!\!E_T$ will point toward a jet. To remove this background, which becomes diminished with increasing $\not\!\!E_T$, we require that the events to satisfy $\Delta\phi/deg + \not\!\!E_T/GeV > 60$, where $\Delta\phi$ is the minimum angle in azimuth between an identified object in the event and the $\not\!\!E_T$.

Both topologies rely on effective identification of hadronic τ decays. Tau lepton identification begins with a jet, which must have one or three charged particles in a 10^0 cone about the jet axis and no additional charged particles in a cone of 30^0. The E_T of the calorimeter cluster must exceed 10 GeV, and the largest P_T of the associated charged particle must exceed 10 GeV/c. Its mass M_τ, which is determined from tracks and electromagnetic calorimeter energy deposits, must be consistent with that of a tau lepton $M_\tau < 1.8$ GeV/c^2. Figure 2 shows the charged track multiplicity distribution for tau candidates in a sample which is enriched in $W^\pm \to \tau\nu + 3$ jets events, which are as complex as $t\bar{t}$ events.

Seven candidate events (all with a τjj$X$ + $\not\!\!E_T$ topology) are observed in 100 pb^{-1} of data, with an expected background of 5.1 ± 1.3 τjj$X$ + $\not\!\!E_T$ events, and 2.2 ± 1.3 ditau events. Most of the background is due to QCD and W, Z + jet(s) events in which a jet mimics ("fakes") the signature of a tau lepton.

For a variety of $H^\pm$ masses, we use the ISAJET v7.06 [9] Monte Carlo program to calculate the efficiency for $t\bar{t} \to WbH\bar{b}$ and $t\bar{t} \to HbH\bar{b}$ events to pass the selection criteria used to find candidate $H^\pm$ events. The total number of expected events is shown as a function of tanβ in Figure 3, for $M_{H^\pm} = 100$ GeV/c^2, and the $t\bar{t}$ cross sections $\sigma_{t\bar{t}} = 5.0$ pb and 7.5 pb. The value of 5.0 pb is the theoretical expectation [10] for the measured top mass of 175 GeV/c^2 [11], while the second value is taken to be 50% larger to illustrate sensitivity

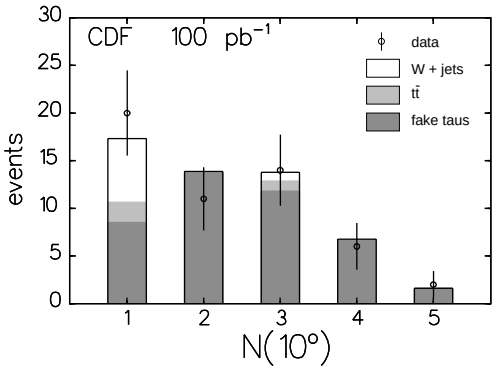

Figure 2: The charged particle multiplicity for tau candidates in the data sample which is collected with the $\not\!\!E_T$ trigger, and used for the direct $H^\pm \to \tau\nu$ search. Cuts have been applied to this sample to enhance the signal from $W^\pm \to \tau\nu + \geq 3$ jets events.

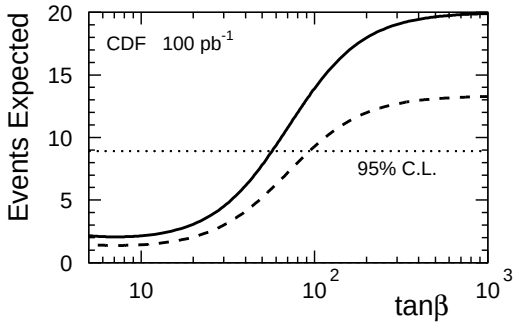

Figure 3: The number of expected events in the direct $H^\pm \to \tau\nu$ search for $M_{H^\pm} = 100$ GeV/c^2 Results are shown for $\sigma_{t\bar{t}} = 5.0$ pb (dashed) and 7.5 pb (solid).

to the assumed value of $\sigma_{t\bar{t}}$. With a 25% systematic uncertainty on the number of expected events, this analysis excludes values of $M_{H^\pm}$ and tanβ for which 8.9 or more signal events are predicted. Figure 4 shows the excluded region in the $M_{H^\pm}$ vs. tanβ plane. For large values of tanβ, $M_{H^\pm} > 147$ GeV/c^2 (158 GeV/c^2) are excluded, assuming $\sigma_{t\bar{t}} = 5.0$ pb (7.5 pb). These results are published in reference [8], where it is shown that additional parameter space can be excluded by taking into account the observed number of SM $t\bar{t}$ decays.

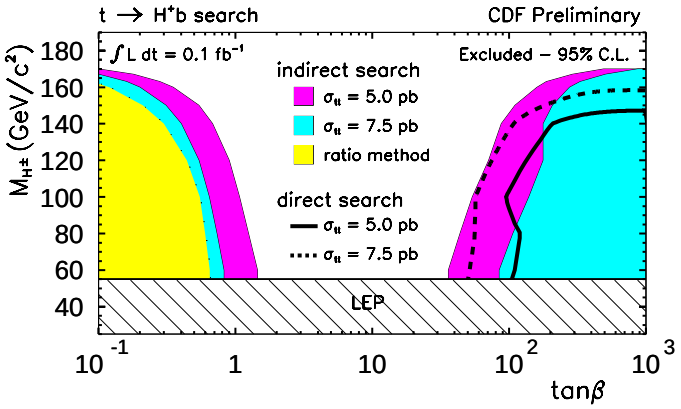

Figure 4: Excluded regions of parameter space in the charged Higgs search. The direct search, for $t\bar{t}$ events which contain at least one $H^{\pm} \to \tau\nu$ decay, excludes the regions at high tanβ to the right of the solid and dashed lines. The indirect search, which uses the results from the top counting experiments, excludes shaded regions at low tanβ and high tanβ. The limits from the direct search are based on observing a deficit of events compared to the number predicted within the two-Higgs-doublet model , and become stronger for a larger assumed $\sigma_{t\bar{t}}$. In contrast, the limits from the indirect search are based on observing an excess of SM $t\bar{t}$ decays, and become weaker with increasing $\sigma_{t\bar{t}}$.

2.2. *Search for $H^{\pm}$ which uses the results from the top counting experiments.*

At low tanβ, where the decay $H^{\pm} \to cs$ is common, a direct search for a dijet mass resonance is difficult. Instead, we examine the effect that the decay mode $t \to H^{\pm}b$ would have on $t\bar{t}$ decay rates to $ee\nu\nu$ + jets, $e\mu\nu\nu$ + jets, and $\mu\mu\nu\nu$ + jets ("dilepton") final states, as well as $e\nu$ + jets and $\mu\nu$ + jets ("lepton + jets") final states. Within the SM, where $t\bar{t}$ decays to $WbW\bar{b}$ nearly 100% of the time, dilepton events are produced primarily when both W bosons decay to $e\nu$ or $\mu\nu$. Lepton + jets events are produced primarily when only one W decays to $e\nu$ or $\mu\nu$, and the other W decays to light quarks.

In each decay channel, the observed number of events is consistent with the expected number of events, assuming that $t\bar{t}$ decays exclusively to $WbW\bar{b}$ [6]. We observe 9 dilepton events and 34 lepton + jets events. Table 1 shows the observed number of signal events after background subtraction of non-$t\bar{t}$ processes in each channel [12]. Also shown is the expected number of events for $\sigma_{t\bar{t}} = 5.0$ pb and 7.5 pb, assuming $\mathcal{B}(t \to W^{\pm}b) = 1.0$.

	dilepton	lepton + jets
$\sigma_{t\bar{t}} = 5.0$ pb	4.1 ± 0.5	20.0 ± 3.0
$\sigma_{t\bar{t}} = 7.5$ pb	6.1 ± 0.7	30.0 ± 4.5
observed	$\mathbf{6.5 \pm 3.0}$	$\mathbf{23.4 \pm 6.0}$

Table 1: Number of expected signal events from $t\bar{t}$ production in the top dilepton channel and the lepton +jets channel, only assuming the decay $t \to W^{\pm}b$. Results are given for two different $t\bar{t}$ cross sections, and are shown with the number of observed events in each channel after background subtraction of non-$t\bar{t}$ processes.

If $\mathcal{B}(t \to H^{\pm}b)$ were large, the $t\bar{t}$ decay rate to each of these two final state topologies would be significantly smaller than the corresponding rate predicted within the SM. This is true whether $H^{\pm}$ decays predominantly to cs or $\tau\nu$. We use the PYTHIA v5.7 [13] Monte Carlo program to find the efficiency for $t\bar{t}$ events with charged Higgs decays to pass the selection cri-

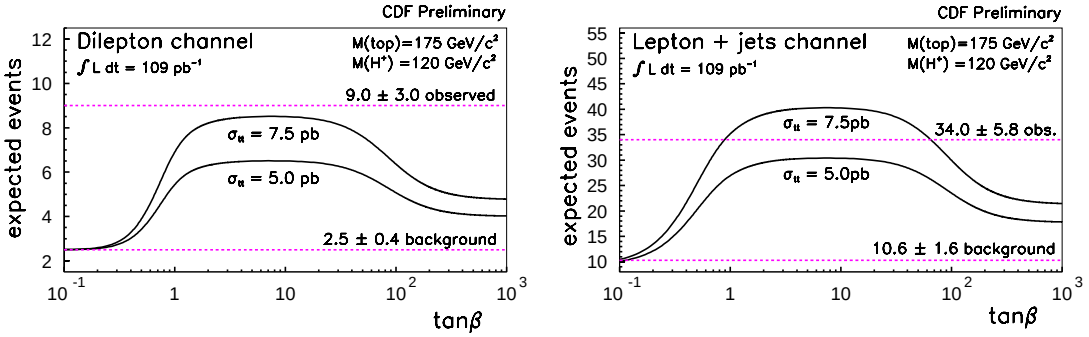

Figure 5: Number of expected events in the dilepton channel (left) and the lepton plus jets channel (right) as a function of tanβ, for $M_{H^\pm} = 120$ GeV/c^2. Results are shown for $\sigma_{t\bar{t}} = 5.0$ pb and 7.5 pb.

teria of the dilepton and lepton + jets channels. For $M_{H^\pm} = 120$ GeV/c^2, Figure 5 plots the number of expected events as a function of tanβ, both for the dilepton channel and the lepton + jets channel. Results are shown for $\sigma_{t\bar{t}} = 5.0$ pb and 7.5 pb.

For tan$\beta \approx 0$, the dominant decay mode for $t\bar{t}$ is $HbH\bar{b}$, where both charged Higgs bosons decay to cs. This all-hadronic final state has a negligible efficiency for passing the selection criteria of either channel, because of the absence of $\not\!\!E_T$ or isolated leptons from $W^\pm$ decay.

For tan$\beta > 30$, $t\bar{t}$ events typically contain one or two $t \to H^\pm b \to \tau\nu b$ decays, which are not as efficient as $t \to W^\pm b$ decays for producing high-P_T electrons or muons. As a result, efficiencies for these events to pass the selection criteria of either channel are reduced from their SM values.

Parameter space is excluded where a significant excess of SM $t\bar{t}$ events is observed above the number that is predicted within the two-Higgs-doublet model. The dilepton and lepton + jets data samples are summed, and treated as a single counting experiment. We exclude values of tanβ, $M_{H^\pm}$ and $\sigma_{t\bar{t}}$ if the probability for finding a total number of events at least as large as the observed number (9+34=43 events) is less than 5%. This probability is calculated from a Poission distribution with a mean equal to the number of expected events for the assumed values of $M_{H^\pm}$ and tanβ. The mean is smeared by a Gaussian that has a width set equal to the total systematic error, which arises from a 12% uncertainty on the number of expected dilepton events and a 16% uncertainty on the number of expected lepton + jets events. Figure 4 shows the excluded region from this analysis in the $M_{H^\pm}$ vs. tanβ plane along with the excluded regions from the direct $H^\pm \to \tau\nu$ search at CDF. Using the theoretical value $\sigma_{t\bar{t}} = 5.0$ pb, we infer that $\mathcal{B}(t \to H^\pm b) < 33\%$ (37%), at the 95% C.L., assuming the decay $H^\pm \to cs$ ($\tau\nu$) dominates. These limits are valid for 60 GeV/$c^2 \leq M_{H^\pm} \leq 170$ GeV/c^2.

To exclude parameter space without assuming a value for $\sigma_{t\bar{t}}$, we measure $\sigma_{t\bar{t}}$ using the observed number of lepton + jets events, and exploit the fact that a large $\mathcal{B}(t \to H^\pm b \to csb)$ suppresses dilepton events more severely than lepton + jets events. This occurs because $t\bar{t}$ decay products $WbW\bar{b}$ and $WbH\bar{b}$ both contribute events to the lepton + jets channel, but only $WbW\bar{b}$ contributes to the dilepton channel. As $\mathcal{B}(t \to H^\pm b) \to 1$, $\mathcal{B}(t\bar{t} \to WbW\bar{b})$

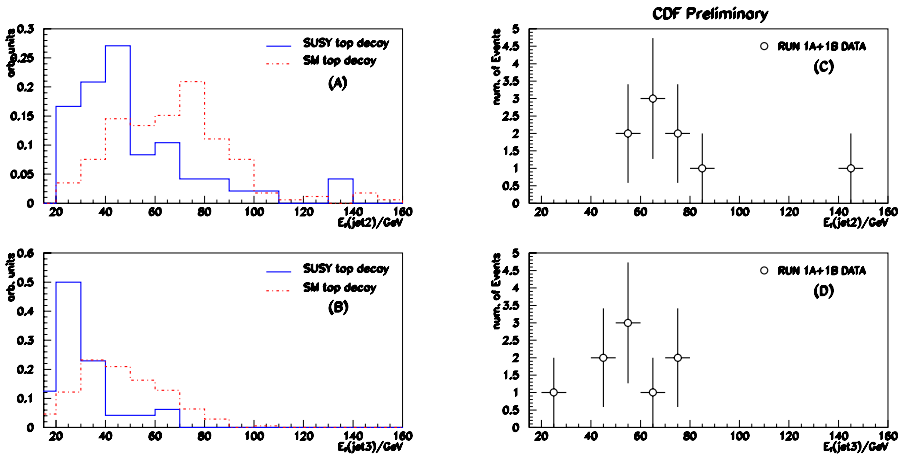

Figure 6: Jet transverse energy distributions for $W^{\pm}$ + $\geq$3 events which have at least one SVX b-tagged jet, and pass the kinematic selection criteria that is designed to enhance a SUSY stop signal and minimize non-$t\bar{t}$ background. The plots in the top row show the jet E_T distributions for the second-highest E_T jet, while plots on the bottom show the jet E_T distribution for the third-highest E_T jet in the events. On the left are Monte Carlo distributions for SM $t\bar{t}$ decays, as well as SUSY $t\bar{t}$ decays which contain at least one $t \to \tilde{t}\tilde{\chi}_1^0$ decay. The corresponding distributions formed by the 9 data events are shown on the right.

decreases much more rapidly than $\mathcal{B}(t\bar{t} \to WbH\bar{b})$, resulting in a ratio of dilepton to lepton + jets events which approaches zero at very small tanβ. In contrast, the ratio observed in the data is 0.27 ± 0.15, which is consistent with the SM value of 0.203 ± 0.041.

First we use the observed number of lepton + jets events to measure $\sigma_{t\bar{t}}$, and then we determine the expected distribution of dilepton events, taking into account $t\bar{t}$ detection efficiencies which are calculated for assumed values of $M_{H^{\pm}}$ and tanβ. These assumed values are excluded if the probability for finding at least the observed number of dilepton events is less than 5%. Figure 4 shows the regions of parameter space excluded at small tanβ, using this "ratio method". We infer $\mathcal{B}(t \to H^{\pm}b) <$ 70% at the 95% C.L., for 60 GeV/$c^2 \leq M_{H^{\pm}} \leq$ 165 GeV/c^2.

To calculate the indirect limits which are described in this section, we assume that no other processes besides $t\bar{t}$ with charged Higgs decays, and other known SM backgrounds, contribute to the dilepton or lepton + jets decay channels.

3. Stop squark search

The large top mass allows top quark's SUSY partners to mix, resulting in one light ($\tilde{t}_1$) and one heavy ($\tilde{t}_2$) mass eigenstate. If $M(\tilde{t}_1) < M_{\rm top}$, then the top quark branching fraction $\mathcal{B}(t \to \tilde{t}_1\tilde{\chi}_1^0)$ could be large. Some models [14] predict $\mathcal{B}(t \to \tilde{t}_1\tilde{\chi}_1^0) \approx 50\%$ and a light chargino with $M(\tilde{\chi}_1^{\pm}) < M(\tilde{t}_1)$, where $\mathcal{B}(\tilde{\chi}_1^{\pm} \to q\bar{q}'\tilde{\chi}_1^0) = 6/9$. We adopt these values, and we also assume an LSP mass $M(\tilde{\chi}_1^0) =$ 20 GeV/c^2. Under these circumstances, most $t\bar{t}$ events would contain one SM top decay, and one SUSY top decay. We search for events where one top quark decays via $t \to W^{\pm}b \to \ell\nu b$, and the other top quark decays via

$$t \to \tilde{t}_1 + \tilde{\chi}_1^0 \to \tilde{\chi}_1^{\pm} + b + \tilde{\chi}_1^0 \to q\bar{q}'\tilde{\chi}_1^0 + b + \tilde{\chi}_1^0 .$$

With the exception of the two LSPs, the result-

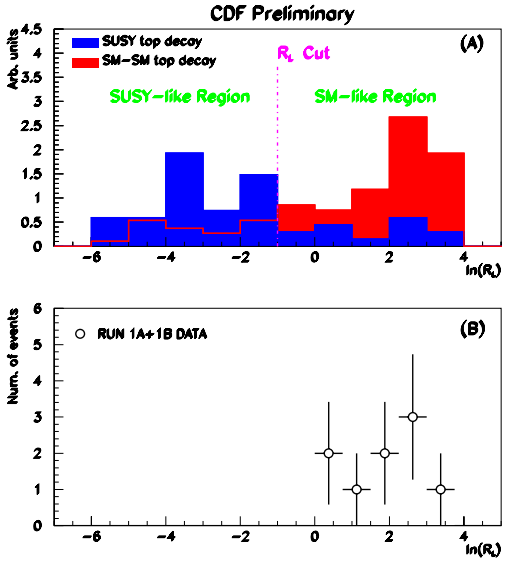

Figure 7: *Top plot:* The quantity $\ln(R_{\mathcal{L}})$ is plotted for a MC sample of SUSY $t\bar{t}$ events, and for a MC sample of SM $t\bar{t}$ events. Most SUSY $t\bar{t}$ events would populate the region $\ln(R_{\mathcal{L}})$ < -1, while most SM $t\bar{t}$ decays should have $\ln(R_{\mathcal{L}})$ > -1. *Bottom plot:* None of the 9 observed events are found in the signal region $\ln(R_{\mathcal{L}})$ < -1.

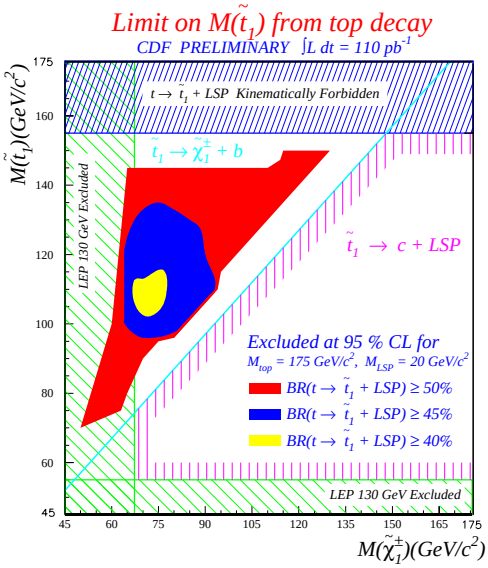

Figure 8: Limits for the process $t \to \tilde{t}_1\tilde{\chi}_1^0$ in the $M(\tilde{t}_1)$ vs. $M(\tilde{\chi}_1^{\pm})$ plane. Results are shown for three different $\mathcal{B}(t \to \tilde{t}_1\tilde{\chi}_1^0)$. Most of the available kinematic parameter space is excluded for $\mathcal{B}(t \to \tilde{t}_1\tilde{\chi}_1^0) \geq 50\%$.

ing $W^{\pm}$ + ≥3 jets final state of $\ell\nu bq\bar{q}'b\tilde{\chi}_1^0\tilde{\chi}_1^0$ has the same topology as a SM $t\bar{t}$ decay to the "lepton + jets" final state $\ell\nu bq\bar{q}'b$. However, the LSPs soften the E_T spectrum of the two jets which originate from the $\tilde{\chi}_1^{\pm}$, compared to the E_T spectrum of jets from the decay of a $W^{\pm}$ boson. This difference between the second- and third-highest E_T jets in the events is exploited to distinguish SUSY $t\bar{t}$ events, which contain at least one $t \to \tilde{t}_1\tilde{\chi}_1^0$ decay, from SM $t\bar{t}$ decays. The strategy of this search is very similar to the one which finds top quark based on the kinematics of the events [15].

First, we create a sample of events which should be enriched in SUSY $t\bar{t}$ decays, and will contain a negligible amount of non-$t\bar{t}$ background. We select $e\nu$ + ≥3 jets events and $\mu\nu$ + ≥3 jets events, where the electron must have E_T > 20 GeV, and the muon must have P_T > 20 GeV/c. We require $\not\!\!E_T$> 45 GeV, which enhances the SUSY signal which contains the two $\tilde{\chi}_1^0$'s. We also require the presence of 2 jets with E_T > 20 GeV and a third jet with E_T > 15 GeV. One jet must originate from a displaced vertex (SVX b-tag). Finally, there must be evidence of a $W^{\pm}$ boson from top quark in the event, in order to reduce the QCD background. The $W^{\pm}$ bosons from QCD processes have a steeply-falling P_T spectrum relative to the P_T spectrum of $W^{\pm}$'s from top decay. We require that $P_T(W^{\pm})$ > 50 GeV/c, where $P_T(W^{\pm})$ is reconstructed from the lepton P_T and the $\not\!\!E_T$. Additional cuts are similar to those in reference [15].

After applying these kinematic selection criteria, and also requiring the SVX b-tag, 9 events remain. The second- and third-highest E_T jets for these 9 events are shown in Figure 6. Also shown are the corresponding Monte Carlo (MC) distributions for SM $t\bar{t}$ events and

SUSY $t\bar{t}$ events. Based on these MC distributions, a quantity called "relative likelihood", $\ln(R_{\mathcal{L}})$, may be formed [15] to determine if an event is more SM-like or SUSY-like, based on its measured jet energies. In Figure 7, this quantity $\ln(R_{\mathcal{L}})$ is plotted for MC samples of SUSY $t\bar{t}$ events and SM $t\bar{t}$ events. Most SUSY $t\bar{t}$ events would populate the region $\ln(R_{\mathcal{L}}) <$ -1 ("SUSY region"), while most SM $t\bar{t}$ decays should have $\ln(R_{\mathcal{L}}) >$ -1 ("SM region"). None of the 9 observed events are found in the signal region $\ln(R_{\mathcal{L}}) <$ -1.

To set limits on stop production, we first generate $t\bar{t}$ events with the ISAJET v7.06 MC program, with constant values for $\mathcal{B}(t \to \tilde{t}_1\tilde{\chi}_1^0)$, $M(\tilde{t}_1)$, and $M(\tilde{\chi}_1^{\pm})$. The $\ln(R_{\mathcal{L}})$ distribution is determined for those events which pass the kinematic selection criteria. We normalize the number of these MC events in the SM region to the observed number of events in that region, to find the number of expected events in the SUSY region. Taking into account systematic errors, the parameter space is excluded at the 95% C.L. if 3.2 events or more are predicted in the SUSY region. Figure 8 shows the excluded region in the $M(\tilde{t}_1)$ vs. $M(\tilde{\chi}_1^{\pm})$ plane, for three assumed values for $\mathcal{B}(t \to \tilde{t}_1\tilde{\chi}_1^0)$. Most of the kinematically allowed parameter space is excluded for $\mathcal{B}(t \to \tilde{t}_1\tilde{\chi}_1^0) \geq 50\%$.

4. Chargino-Neutralino search

A trilepton + $\not\!\!E_{\rm T}$ signature which has a very small SM background arises from direct production of chargino-neutralino pairs, followed by their subsequent decay into leptons,

$$p\bar{p} \;\to\; \tilde{\chi}_1^{\pm}\tilde{\chi}_2^0 \;\to\; (\ell^{\pm}\nu\tilde{\chi}_1^0)(\ell^{\pm}\ell^{\pm}\tilde{\chi}_1^0)\,.$$

The $\tilde{\chi}_1^{\pm}$ and $\tilde{\chi}_2^0$ decays are mediated by virtual $W^{\pm}$s and Z^0s, and virtual sleptons. The masses of the sleptons are related to the squark and gluino masses according to the predictions of SUGRA-inspired models [16].

Candidate events must contain an e^+e^- or $\mu^+\mu^-$ pair, a third lepton, and $\not\!\!E_{\rm T} > 15$ GeV. One lepton must have $E_T > 11$ GeV and pass tight identification requirements, while the other two leptons must have $E_T > 5$ GeV and pass looser identification cuts. Events with opposite-charge leptons which are consistent with J/ψ, Υ, or Z^0 resonances are removed. Before requiring $\not\!\!E_{\rm T}>$ 15 GeV, 8.0 $\pm$ 1.6 background events are expected and 7 are observed in 107 pb^{-1} of data. After requiring $\not\!\!E_{\rm T}>$ 15 GeV, 1.2 $\pm$ 0.24 background events are expected, and 0 are observed. Most of the background is due to Drell-Yan dilepton events which contain a third "fake" lepton from a jet, a decay-in-flight, or an underlying event.

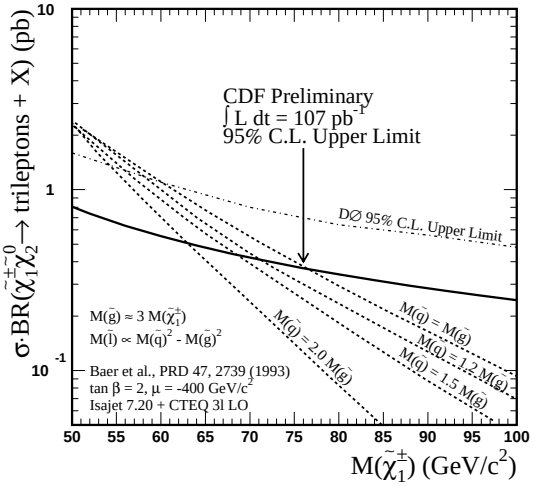

Figure 9: Values of $\sigma(p\bar{p} \to \tilde{\chi}_1^{\pm}\tilde{\chi}_2^0) \cdot \mathcal{B}(\tilde{\chi}_1^{\pm}\tilde{\chi}_2^0 \to$ trileptons + $\not\!\!E_{\rm T}$) which are excluded by this analysis lie above the 95% C.L. upper limit line. Theoretical values for $\sigma \cdot \mathcal{B}$ are plotted for several values of $M(\tilde{q})/M(\tilde{g})$. These results are valid for tanβ = 2 and μ = -400 GeV/c^2. Our best limit is $M(\tilde{\chi}_1^{\pm}) >$ 81.5 GeV/c^2, for $M(\tilde{q}) = M(\tilde{g})$, tan$\beta$ = 2 and μ = -600 GeV/c^2.

This analysis excludes $\sigma(p\bar{p} \to \tilde{\chi}_1^{\pm}\tilde{\chi}_2^0) \cdot \mathcal{B}(\tilde{\chi}_1^{\pm}\tilde{\chi}_2^0 \to$ trileptons + $\not\!\!E_{\rm T}$) which are large enough to predict at least 3.2 trilepton events. This 95% C.L. upper limit on $\sigma \cdot \mathcal{B}$ is shown as a function of $M(\tilde{\chi}_1^{\pm})$ in Figure 9, for tanβ

= 2, and μ = -400 GeV/c^2. This limit improves with increasing $\tilde{\chi}_1^{\pm}$ mass, since higher-mass $\tilde{\chi}_1^{\pm}$s (and hence, higher-mass $\tilde{\chi}_2^0$s) decay to more energetic leptons which have increased efficiency for satisfying the lepton E_T requirements. Also shown in Figure 9 are the theoretical predictions for $\sigma \cdot \mathcal{B}$ from the ISAJET v7.20 Monte Carlo program for several squark-gluino mass ratios. Not shown is our best limit $M(\tilde{\chi}_1^{\pm}) > 81.5$ GeV/c^2 ($\sigma \cdot \mathcal{B} < 0.35$), for $M(\tilde{q})$ = $M(\tilde{g})$, tanβ = 2, and μ = -600 GeV/c^2.

The limits become diminished with increasing $M(\tilde{q})/M(\tilde{g})$. As $M(\tilde{q})$ increases, $\sigma(p\bar{p} \rightarrow \tilde{\chi}_1^{\pm}\tilde{\chi}_2^0)$ increases because a t-channel virtual $\tilde{q}$ exchange diagram, which interferes destructively with the s-channel $W^{\pm}$ exchange diagram for $\tilde{\chi}_1^{\pm}\tilde{\chi}_2^0$ production, becomes suppressed. However, as $M(\tilde{q})/M(\tilde{g})$ increases, this effect is overshadowed by an increase in the slepton masses, resulting in decreased branching fractions of the $\tilde{\chi}_1^{\pm}$ and $\tilde{\chi}_2^0$ to leptons.

5. Searches for *R*-parity violating squark and LSP decays

The excess of high-Q^2 events observed at H1 [17] and Zeus [18] may indicate the presence of a resonance corresponding to a mass of 200 GeV/c^2. It has been proposed [19,20] that within the framework of the MSSM, these events could arise from the $\not{R}_p$ production and decay of the charm squark, $ed \rightarrow \tilde{c}_L \rightarrow ed$. An R_p-conserving charm squark decay followed by an $\not{R}_p$ LSP decay, $\tilde{c}_L \rightarrow c(\tilde{\chi}_1^0 \rightarrow q\bar{q}'e)$, could have a branching fraction comparable to the $\tilde{c}_L \rightarrow ed$ decay that is hypothesized to have been observed [21]. We search for both of these decays at CDF, which proceed through a lepton-number violating coupling λ'_{121} [19,20].

5.1. *Search for $\tilde{c}_L \rightarrow ed$*

At the Tevatron, we search for gluino pair production, followed by the decay

$$\tilde{g}\tilde{g} \rightarrow (\bar{c}\tilde{c}_L)(\bar{c}\tilde{c}_L) \rightarrow (\bar{c}e^+d)(\bar{c}e^+d) \text{ or } c.c.,$$

where "c.c." denotes the "charge-conjugated" state, and $M(\tilde{c}_L) = 200$ GeV/c^2. A like-charge electron + jets signature with a small SM background is expected in 1/2 of all these decays which contain ee in the final state, because the gluino decays to $\bar{c}\tilde{c}_L$ and its charge-conjugate state $c\bar{\tilde{c}}_L$ with equal probability. The charm squark does not decay into the $\tilde{\chi}_1^{\pm}$ or $\tilde{\chi}_1^0$ since it is assumed that $M(\tilde{\chi}_1^{\pm})$, $M(\tilde{\chi}_1^0) > M(\tilde{c}_L)$.

Candidate events must contain 2 like-charge isolated electrons with $E_T > 15$ GeV and 2 jets with $E_T > 15$ GeV. We also reject events which contain a significant amount of $\not{E}_T$, in contrast to most searches for R_P-conserving decays which are expected to produce an LSP that is stable and escapes detection. No events are observed in 105 pb^{-1} of data, which is consistent with background estimates from $t\bar{t}$, $b\bar{b}$ and $c\bar{c}$ production.

With a signal efficiency of about 15% for

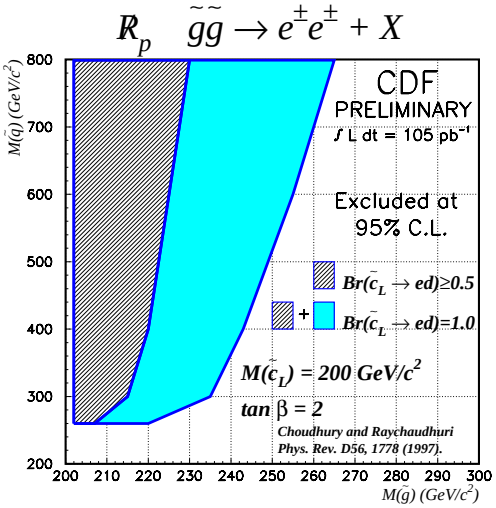

Figure 10: Excluded regions for the R_p-violating squark decay $\tilde{c}_L \rightarrow ed$ in the degenerate squark mass vs. gluino mass plane, if $M(\tilde{c}_L) = 200$ GeV/c^2.

a large range of $M(\tilde{g})$, we find $\sigma(p\bar{p} \to \tilde{g}\tilde{g}) \cdot \mathcal{B}(\tilde{g}\tilde{g} \to e^{\pm}e^{\pm} + X) > 0.19$ pb at the 95% C.L. We exclude parameter space if this value of 0.19 pb is lower than the next-to-leading order (NLO) theoretical $\tilde{g}\tilde{g}$ cross section [22] multiplied by its theoretical branching fraction to like-charge dielectrons [19]. In Figure 10, the excluded region is shown in the $M(\tilde{q})$ vs. $M(\tilde{g})$ plane, for $\mathcal{B}(\tilde{c}_L \to ed) = 0.5$ and 1.0. The value $\mathcal{B}(\tilde{c}_L \to ed) = 1.0$ is preferable to explain the HERA results. However, the null result in the CDF [23] and DØ [24] searches for the first-generation leptoquark $LQ1$, with $\mathcal{B}(LQ1 \to ed) = 1.0$ and $M(LQ1) = 200$ GeV/c^2, motivates the value $\mathcal{B}(\tilde{c}_L \to ed) = 0.5$, since the production and decay of $LQ1$ and $\tilde{c}_L$ are assumed to be kinematically identical at HERA.

At high degenerate squark mass $M(\tilde{q})$, the gluino only decays to $\bar{c}\tilde{c}_L$, while for lower $M(\tilde{q})$, the gluino decays to other squark flavors as well. However, in the assumed model, only the $\tilde{c}_L$ has the $\not{R}_{\rm p}$ coupling that allows like-charge electrons in the final state. This explains the degradation in the limit with decreasing $M(\tilde{q})$ for constant $M(\tilde{g})$, shown in Figure 10. Our sensitivity vanishes for $M(\tilde{q})$ < 260 GeV/c^2, where $M(\tilde{b}_L)$ becomes lighter than 200 GeV/c^2, and the decay $\tilde{g} \to \bar{b}\tilde{b}_L$ dominates over the decay $\tilde{g} \to \bar{c}\tilde{c}_L$.

5.2. *Search for* $\tilde{\chi}_1^0 \to q\bar{q}'e^{\pm}$

It has been shown [21] that the R_p-conserving decay $\tilde{c}_L \to c\tilde{\chi}_1^0$ can compete with the R_p-violating decay $\tilde{c}_L \to ed$ which was just described. According to the model proposed in reference [21], a like-charge dielectron signal could arise from

$$p\bar{p} \to \tilde{c}_L\bar{\tilde{c}}_L \overset{R_{\rm p}}{\to} c\tilde{\chi}_1^0\bar{c}\tilde{\chi}_1^0 \overset{\not{R}_{\rm p}}{\to} c(q\bar{q}'e^{\pm})\bar{c}(q\bar{q}'e^{\pm})$$

where the $\tilde{c}_L$ decay conserves R-parity, while the $\tilde{\chi}_1^0$ decay violates R-parity. If we assume that $\mathcal{B}(\tilde{c}_L \to c\tilde{\chi}_1^0) = 1.0$, and $\mathcal{B}(\tilde{\chi}_1^0 \to q\bar{q}'e^{\pm})$ = 0.5 (the $\tilde{\chi}_1^0$ also decays to neutrinos), then these decays will result in a like-charge dielectron + jets signature 1/8 of the time. Events are required to satisfy the same selection criteria which are applied for the $\tilde{c}_L \to ed$ search.

It is assumed that

$$M(\tilde{\chi}_1^{\pm}) > M(\tilde{c}_L) > M(\tilde{\chi}_1^0),\ M(\tilde{\chi}_1^{\pm}) \approx 2 \cdot M(\tilde{\chi}_1^0)$$

where the first relation suppresses charm squark decays to a chargino, and the second relation arises from gaugino mass unification. Thus, for a set value of $M(\tilde{c}_L)$, we are sensitive to $\tilde{\chi}_1^0$ masses in the range $M(\tilde{c}_L)/2 < M(\tilde{\chi}_1^0) < M(\tilde{c}_L)$ - $M(c)$.

We calculate, for each charm squark and neutralino mass, the upper limit cross section times branching fraction to like-charge electrons. We compare our results with theoretical predictions in Figure 11. Our 95% C.L. upper limits are plotted as a function of $M(\tilde{c}_L)$, for the lightest and heaviest values of $M(\tilde{\chi}_1^0)$ which are allowed. We are sensitive to a smaller $\sigma \cdot \mathcal{B}$ for the heavier neutralino, which produces a harder electron E_T spectrum resulting in an increased efficiency for satisfying the electron E_T requirement. Also shown is the leading-order $\tilde{c}_L\bar{\tilde{c}}_L$ cross section from the ISAJET v7.06 program, multiplied by a branching fraction of 1/8. Our sensitivity lies just below $M(\tilde{c}_L) =$ 150 GeV/c^2.

Next, we make the assumption that 5 degenerate squarks can decay via

$$p\bar{p} \to \tilde{q}\bar{\tilde{q}} \overset{R_{\rm p}}{\to} q\tilde{\chi}_1^0\bar{q}\tilde{\chi}_1^0 \overset{\not{R}_{\rm p}}{\to} q(q\bar{q}'e^{\pm})\bar{q}(q\bar{q}'e^{\pm}) .$$

Neutralino production will be enhanced from the decays of 10 different squark-antisquark pairs (5 flavors × 2 helicities). The corresponding theoretical NLO $\tilde{q}\bar{\tilde{q}}$ cross section [25], multiplied by a branching ratio of 1/8, is shown along with the 95% C.L. upper limit curves from our analysis in Figure 12. The NLO cross section exhibits a gluino mass dependence, due to gluino exchange diagrams for u

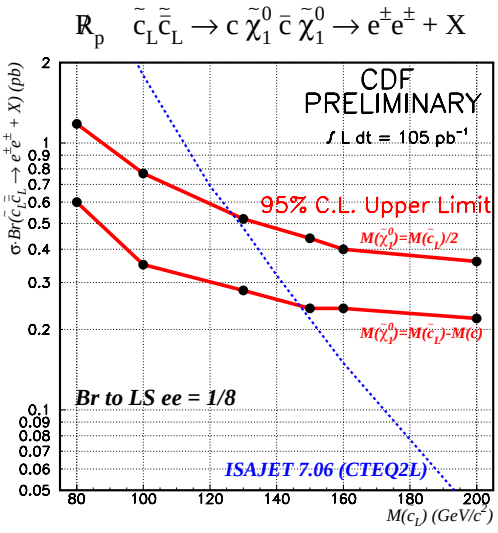

Figure 11: Upper limits for $\sigma(p\bar{p} \to \tilde{c}_L\bar{\tilde{c}}_L) \cdot \mathcal{B}(\tilde{c}_L\bar{\tilde{c}}_L \to e^{\pm}e^{\pm} + X)$ in the search for lepton-number violating LSP decays. "X" contains at least 2 jets. The decay $\tilde{c}_L \to c\tilde{\chi}_1^0$ is allowed only if the value of $M(\tilde{\chi}_1^0)$ lies between the two curves. Also shown is the leading-order $\sigma(p\bar{p} \to \tilde{c}_L\bar{\tilde{c}}_L)$ prediction from ISAJET multiplied by a factor of 1/8, which is the maximum expected branching fraction for $\tilde{c}_L\bar{\tilde{c}}_L$ decay to like-charge electrons. The $\mathcal{B}(\tilde{c}_L \to c\tilde{\chi}_1^0)$ is assumed to be 1.0.

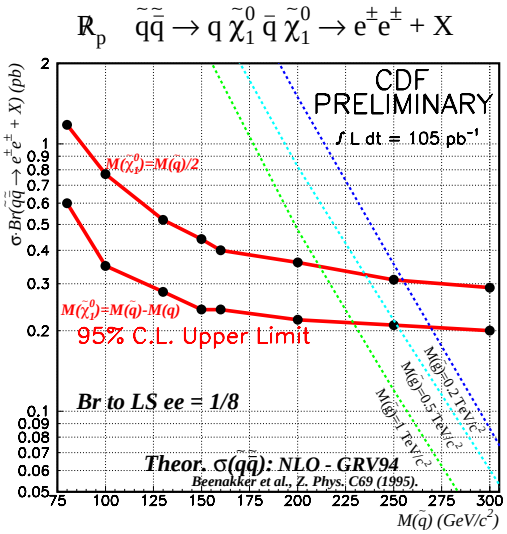

Figure 12: This plot contains the same experimental upper limits shown in Figure 11. However, now we assume that 5 degenerate squark flavors can decay via $\tilde{q} \to q\tilde{\chi}_1^0 \to qq\bar{q}'e$. Also shown is the NLO cross section $\sigma(\tilde{q}\bar{\tilde{q}})$ calculated for three different values of $M(\tilde{g})$, and multiplied by a branching fraction of 1/8. Our sensitivity is substantially increased, and we exclude degenerate squark masses between 210 and 270 GeV/c^2 depending upon the $M(\tilde{g})$ and $M(\tilde{\chi}_1^0)$. The $\mathcal{B}(\tilde{q} \to q\tilde{\chi}_1^0)$ is assumed to be 1.0.

and d quarks. We set gluino and neutralino mass-dependent lower limits on the degenerate squark mass between 210 and 270 GeV/c^2. We note that these limits are determined using $\mathcal{B}(\tilde{q} \to q\tilde{\chi}_1^0) = 1.0$, whereas $\mathcal{B}(\tilde{c}_L \to ed)$ must be appreciable to explain the HERA results. However, even allowing for this, our analysis is still sensitive to the region of 200 GeV/c^2, depending on the values of $M(\tilde{g})$ and $M(\tilde{\chi}_1^0)$.

6. Conclusions

No evidence for supersymmetric particle production is observed. Values of $M_{H^{\pm}}$ as large as 170 GeV/c^2 have been excluded for large $\mathcal{B}(t \to H^{\pm}b)$. For $\tilde{t}_1$, we exclude most of the allowed parameter space if $\mathcal{B}(t \to \tilde{t}_1\tilde{\chi}_1^0) \geq 50\%$, assuming $M(\tilde{\chi}_1^0) = 20$ GeV/c^2. Our best limit on the chargino mass is $M(\tilde{\chi}_1^{\pm}) >$ 81.5 GeV/c^2, assuming $M(\tilde{q}) = M(\tilde{g})$, tan$\beta$ = 2, and μ = -600 GeV/c^2. Assuming that $\mathcal{B}(\tilde{c}_L \to ed) = 0.5$, we can exclude $M(\tilde{c}_L) =$ 200 GeV/c^2. We also search for the competing decay $\tilde{c}_L \to c(\tilde{\chi}_1^0 \to q\bar{q}'e^{\pm})$, and exclude $M(\tilde{c}_L)$ as large as 140 GeV/c^2. Finally, if 10 degenerate squarks decay via $\tilde{q} \to q(\tilde{\chi}_1^0 \to q\bar{q}'e^{\pm})$, then we exclude $M(\tilde{q}) < 215$ GeV/c^2.

Currently CDF continues to analyze Run I data. We are also upgrading the detector for Run II, scheduled to begin in the year 2000. The upgraded Tevatron will have a center-of-mass energy of $\sqrt{s}$ = 2.0 TeV and an instantaneous luminosity of $\mathcal{L} \approx 2 \times 10^{32}$ cm^{2}s^{-1}. During the first two years of running, about 2 fb^{-1} of data should be collected, which is almost a 20-fold increase in the present data set.

7. Acknowledgments

Thanks to Maxwell Chertok, Leslie Groer, Carmine Pagliarone, and Benn Tannenbaum for explaining these analyses to me, and for their plots which appear here. David Stuart was helpful in preparing this talk.

We thank the Fermilab staff and technical staffs of the participating institutions for their vital contributions.

8. References

1. CDF Collaboration, F. Abe *et al.*, Phys. Rev. D **56** 1357 (1997).
2. CDF Collaboration, F. Abe *et al.,* Phys. Rev. Lett. **76** 2006 (1996); J. Done, for the CDF Collaboration, *Search for Squarks and Gluinos using Dileptons*, FERMILAB-CONF-96-372-E, talk presented at the 1996 Annual Divisional Meeting (DPF 96) of the Division of Particles and Fields of the American Physical Society, Minneapolis, MN, 10-15 Aug 1996.
3. R. Culbertson, for the CDF and D0 Collaborations, *SUSY Searches at the Tevatron*, FERMILAB-CONF-97-277-E, to be published in the proceedings of 5th International Conference on Supersymmetries in Physics (SUSY 97), Philadelphia, PA, 27-31 May 1997.
4. L. Groer, for the CDF and D0 Collaborations, *Present Searches for Higgs Signatures at the Tevatron*, FERMILAB-CONF-97-213-E, talk presented at the 12th Workshop on Hadron Collider Physics (HCP 97), Stony Brook, NY, 5-11 Jun 1997 (hep-ex/9707034).
5. CDF Collaboration, F. Abe *et al.,* Nucl. Instrum. Meth. **A271**, 387 (1988).
6. CDF Collaboration, F. Abe *et al.*, *Measurement of the $t\bar{t}$ Production Cross Section in $p\bar{p}$ Collisions at $\sqrt{s}$ = 1.8 TeV*, FERMILAB-PUB-97-286-E, submitted to Phys. Rev. Lett. (hep-ex/9710008).
7. J. Gunion *et al.,* The Higgs Hunter's Guide (Addison-Wesley, New York, 1990); M. Drees and D.P. Roy, Phys. Lett. B **269**, 155 (1991).
8. CDF Collaboration, F. Abe *et al.,* Phys. Rev. Lett. **79** 357 (1997).
9. H. Baer, et al., in *Proceedings of the Workshop on Physics at Current Accelerators and the Supercollider*, Argonne, 1993, edited by J. Hewett, A. White and D. Zeppenfeld (Argonne National Laboratory, Argonne, Illinois, 1993), p. 703 (hep-ph/9305342).
10. E. Laenen, J. Smith, and W.L. van Neerven, Phys. Lett. B **321**, 254 (1994).
11. D0 Collaboration, S. Abachi *et al.*, Phys. Rev. Lett. **79**, 1197 (1997); CDF Collaboration, F. Abe *et al.*, *Measurement of the Top Quark Mass*, FERMILAB-PUB-97-284-E, submitted to Phys. Rev. Lett.
12. The non-$t\bar{t}$ backgrounds used in the charged Higgs analysis are slightly higher than those found in reference [6], where the portion of the background which is calculated from data is corrected for its top content, assuming $\mathcal{B}(t \to W^+b) = 1.0$. Such a correction is not performed for the charged Higgs search.
13. T. Sjöstrand, Comput. Phys. Commun. **82**, 74 (1994).
14. G.L. Kane and J. Wells, Phys. Rev. Lett, **76** 869 (1996); J. Sender, *Light $\tilde{t}_1 \to \tilde{W}_1 b$ Models are Not Ruled Out by Tevatron Top Experiments*, University of Hawaii preprint UH-511-843-96, (1996) (hep-ph/9602354).
15. CDF Collaboration, F. Abe *et al.,* Phys. Rev. **D51** 4623 (1995).
16. M. Drees and M. Nojiri, Nucl. Phys. **B369**, 54 (1992); H. Baer *et al.,* Phys. Rev. **D47**, 2739 (1992).
17. C. Adloff *et al.,* Z. Phys. **C74** 191 (1997).
18. J. Breitweg *et al.,* Z. Phys. **C74** 207 (1997).
19. D. Choudhury and S. Raychaudhuri, Phys. Rev. **D56** 1778 (1997).
20. J. Butterworth, H. Dreiner, Nucl. Phys. **B397** 3 (1993).
21. G. Altarelli *et al.*, *Pursuing Interpretations of the HERA Large Q^2 Data*, CERN-TH-97-040, (1997) (hep-ph/9703276).
22. W. Beenakker *et al.*, Z. Phys. **C69** 163 (1995).
23. CDF Collaboration, F. Abe *et al.*, *Search for First Generation Leptoquark Pair Production in $\bar{p}p$ Collisions at $\sqrt{s}$ = 1.8 TeV*, FERMILAB-PUB-97-280-E, submitted to Phys. Rev. Lett. (hep-ex/9708017).
24. D0 Collaboration, B. Abbott *et al.*, *Search for Scalar Leptoquark Pairs Decaying to Electrons and Jets in $p\bar{p}$ Collisions*, FERMILAB-PUB-97-252-E, submitted to Phys. Rev. Lett. (hep-ex/9707033).
25. W. Beenakker *et al.,* Nucl. Phys. **B492** 51 (1997).